

Data Science-Enabled Palladium-Catalyzed Enantioselective Aryl-Carbonylation of Sulfonimidamides

Lucy van Dijk,[#] Brittany C. Haas,[#] Ngiap-Kie Lim,* Kyle Clagg, Jordan J. Dotson, Sean M. Treacy, Katarzyna A. Piechowicz, Vladislav A. Roytman, Haiming Zhang, F. Dean Toste,* Scott J. Miller, Francis Gosselin, and Matthew S. Sigman*



Cite This: <https://doi.org/10.1021/jacs.3c06674>



Read Online

ACCESS |

Metrics & More

Article Recommendations

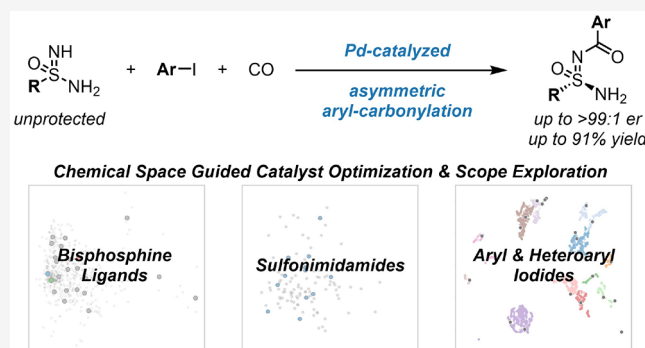
Supporting Information

ABSTRACT: New methods for the general asymmetric synthesis of sulfonimidamides are of great interest due to their applications in medicinal chemistry, agrochemical discovery, and academic research. We report a palladium-catalyzed cross-coupling method for the enantioselective aryl-carbonylation of sulfonimidamides. Using data science techniques, a virtual library of calculated bisphosphine ligand descriptors was used to guide reaction optimization by effectively sampling the catalyst chemical space. The optimized conditions identified using this approach provided the desired product in excellent yield and enantioselectivity. As the next step, a data science-driven strategy was also used to explore a diverse set of aryl and heteroaryl iodides, providing key information about the scope and limitations of the method. Furthermore, we tested a range of racemic sulfonimidamides for compatibility of this coupling partner. The developed method offers a general and efficient strategy for accessing enantioenriched sulfonimidamides, which should facilitate their application in industrial and academic settings.

INTRODUCTION

The discovery of sulfonamides revolutionized medicine with life-saving antibiotics in the 1930's,¹ with now >150 marketed drugs including this pharmacophore, which showcase a broad spectrum of biological activities.² More recently, sulfonimidamides, a chiral bioisostere of sulfonamides, have emerged and received significant attention due to their increased ability to modulate physicochemical properties provided by the additional *N*-substituent (Figure 1A).^{3–6} The racemic synthesis of sulfonimidamides generally proceeds through functionalization of sulfonamides and sulfonamides, among other methods,^{7,8} and stereospecific methods to access enantioenriched sulfonimidamides have been reported from enantioenriched sulfonimidoyl chlorides⁹ and fluorides (Figure 1B).^{10,11} The asymmetric synthesis of enantioenriched sulfonimidamides has been reported via Rh-catalyzed kinetic resolution¹² along with organocatalyzed transformations.^{13–15} However, these methods are limited with regard to the substrate scope and further functionalization of the final product. Therefore, we sought to develop a general method to access enantioenriched sulfonimidamides.

In this context, we hypothesized that the dynamically equilibrating tautomers of unprotected sulfonimidamides could provide an opportunity for the selective interception of the desired enantiomer to afford an asymmetric transformation.



This unusual feature of the sulfonimidamide functional group was first exploited in asymmetric synthesis by Willis and co-workers when they reported the dynamic kinetic resolution of an enantiotopic nitrogen via alkylation of protected, racemic sulfonimidamides (Figure 1B).

This process is catalyzed by a cinchona alkaloid-derived quaternary ammonium phase-transfer catalyst to allow direct access to enantioenriched products.¹³ Motivated by this result, we posited that a Pd-catalyzed carbonylative cross-coupling of sulfonimidamides, inspired by the reports from Sandström, Arvidsson, and co-workers (Figure 1C),^{16,17} with a library of commercially available electrophiles would provide access to a range of enantiomerically enriched sulfonimidamides.

Herein, we set out to develop this reaction (Figure 1D) by applying a data science-guided reaction optimization and scope exploration. Our recently reported virtual library of calculated bisphosphine ligand descriptors¹⁸ enabled the effective sampling of catalyst chemical space with the aim of shortening

Received: June 24, 2023

Published: September 1, 2023

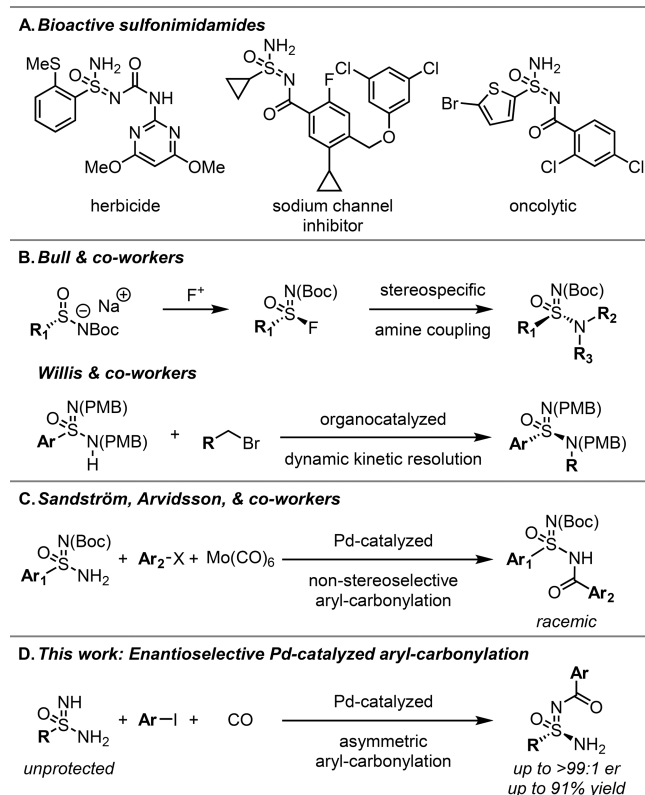


Figure 1. Application and synthesis of sulfonimidamides. (A) Bioactive sulfonimidamide compounds. (B) Previously published syntheses of enantioenriched sulfonimidamides. (C) Nonstereospecific synthesis of racemic acyl sulfonimidamides via Pd-catalyzed aryl-carbonylation. (D) This work: asymmetric synthesis of acyl sulfonimidamides via Pd-catalyzed aryl-carbonylation with aryl and heteroaryl iodides.

optimization timelines and increasing the possibility of locating a global optimum.^{19–21} Data science techniques were also employed for substrate scope selection in order to maximize chemical space exploration, thus assessing the generality of this method.^{22,23}

■ RESULTS AND DISCUSSION

Reaction Optimization. We commenced our investigation into the development of a Pd-catalyzed carbonylative arylation of sulfonimidamides by examining Pd(bisphosphine)-catalysts with phenylsulfonimidamide **1a** and 1-iodonaphthalene **2a** as model coupling partners (Figure 2A). To guide our initial efforts, we designed a screening set of chiral bisphosphine ligands, which reflects the optimal diversity of the commercially available bisphosphine ligand chemical space. To accomplish this, we utilized our recently reported library of calculated bisphosphine ligand descriptors and chemical space representation.¹⁸ This provided the framework for a relatively unbiased selection of initial ligands, by defining the bisphosphine chemical space into a specified number of discrete clusters using the k-means clustering algorithm with the hyperparameter “k” set to the number of experiments planned for the first high-throughput experimentation (HTE) plate (Figure 2B).²¹ The selection of the 24 ligands (Figure 2C) was curated for availability in the Genentech ligand library as well as cost. This protocol could be viewed as a designed training set for a range of downstream screening and data science

objectives, especially for other transition-metal(bisphosphine)-catalyzed asymmetric reactions, in which limited prior knowledge of compatible ligands is known. This set of 24 diverse ligands was used in a HTE screening campaign (using 1 solvent and 3 bases—see [SI](#) for details), which led to the identification of several high performing examples highlighted by the top performing reaction using Mandyphos ligand SL-M003-1 (100% conversion, 96:4 er).^{24,25} Two axially chiral biaryl ligands, (*R*)-C3-TunePhos²⁶ and (*S*)-3,5-Xyl-MeOBI-PHEP,²⁷ also displayed good conversion and enantioselectivity (59–80% conversion, 89:11 and 90:10 er). To probe if an improved ligand could be identified, we turned to chemical space analysis, wherein commercially available ligands proximal to SL-M003-1 and the other top-performing ligands were evaluated. This screen revealed that Mandyphos SL-M003-1 remained the best ligand for the model substrate (see [SI](#) for details).

Through validation of the HTE results on benchtop scale, we found premixing of the precatalyst and ligand in solution before adding to the reaction mixture favored a more consistent and chemoselective (formation of the monoacylated product **3aa**) cross-coupling. With this setup, the best conditions from the HTE screen (Mandyphos SL-M003-1 ligand, Et₃N base, and TBME solvent) were repeated on a 1.0 mmol scale to confirm the high conversion and enantioselectivity (100% conversion, 90:10 er). Additionally, the reaction profile was remarkably clean, with 96% conversion to desired product **3aa** and bis-acylated product **4aa** as the only side product observed (from SFC analysis, [Table 1](#), entry 1). The direct cross-coupling product was not observed in the presence of CO. In preliminary exploration of the chemistry, we briefly evaluated the effect of temperature. Higher reaction temperatures (up to 50 °C) were found to lead to higher conversions for some electrophiles, but the reaction profiles were not as clean. Lower reaction temperatures did not provide improved selectivity. Hence, a moderate reaction temperature (20 °C) was selected for practicality and ease of setup in a high-pressure vessel. Other bases, such as 2-(dimethylamino)-ethyl ether (DMAEE) and 4-methylmorpholine (NMM) were also evaluated and confirmed to lead to lower enantioselectivity (85:15 and 80:20 er, respectively). Considering the sensitivity of base selection, we further explored this variable and found that using *N,N*-diisopropylethylamine (DIPEA) as a base improved the selectivity to 94:6 er. Inorganic bases (K₂CO₃ and *t*-BuOK) were also explored but only provided the desired coupling product **3aa** in <15% conversion (by SFC analysis). Additionally, the evaluation of alternative solvents revealed that toluene provided higher enantioselectivity for the coupling (96:4 er), although the chemoselectivity was slightly reduced (11% of **4aa**). Under these optimized reaction conditions ([Table 1](#), entry 8), (*R*)-**3aa** was obtained in 84% isolated yield, which allowed us to determine the absolute configuration unambiguously by an X-ray crystallographic analysis.

Electrophile Scope Exploration. As the next step, a data science-driven approach was exploited to design a comprehensive electrophile set, which would quantitatively cover chemical space, in order to rigorously explore the scope and limitations of this transformation. This approach has been recently employed for various applications including Ni/photoredox-catalyzed²² and amide coupling^{23,28} reactions, following a similar strategy to that described above for bisphosphine selection. Similarly, Doyle and Sigman recently

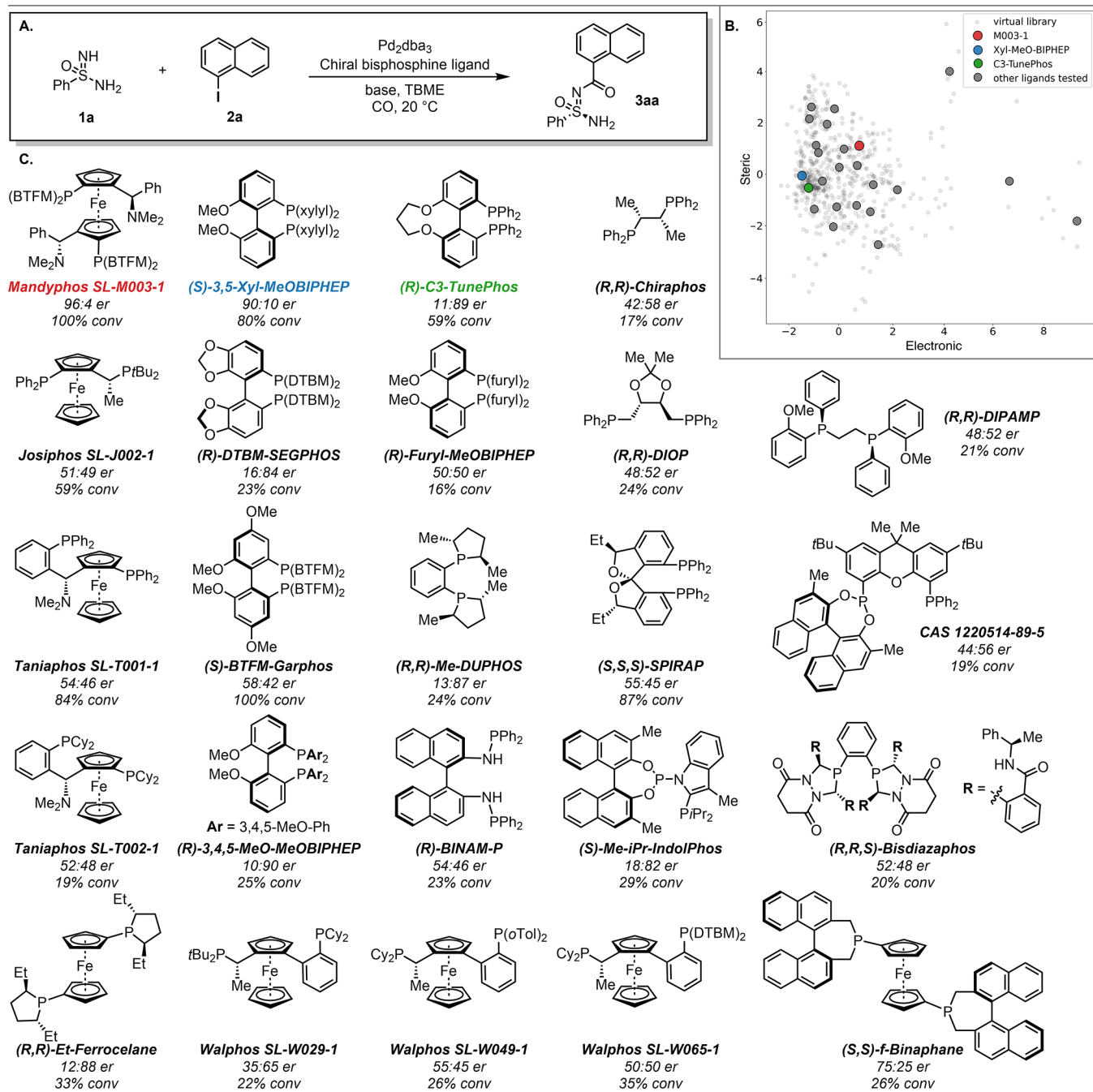


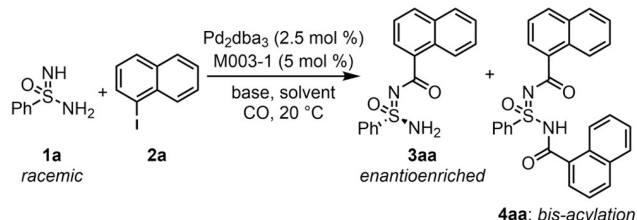
Figure 2. Bisphosphine ligand training set design. (A) Model system for the development of a Pd-catalyzed enantioselective aryl-carbonylation of sulfonimidamides. TBME = methyl *tert*-butyl ether. (B) A bisphosphine chemical space map showing the set of 24 ligands designed to encompass the diversity of bisphosphine chemical space. The top three ligands are highlighted on this stereoelectronic map. (C) The structures of the selected ligands are shown along with results of the initial exploratory catalyst screen with the Et_3N base in TBME solvent. BTFM = 3,5-bis(trifluoromethyl)phenyl, DTBM = 3,5-di-*tert*-butyl-4-methoxyphenyl.

reported a library of DFT-level molecular descriptors for commercially available aryl iodides, which they applied to the design of a representative aryl iodide set to interrogate Ni(1)-mediated oxidative addition.^{29,30} Here, we used the conserved molecular descriptors from the aryl and heteroaryl iodide libraries to construct a uniform manifold approximation and projection (UMAP) representation of >5000 commercially available examples (Figure 3B). Hierarchical clustering was subsequently employed to partition the library of electrophiles into 13 clusters (see SI for details). Examples from each cluster

were selected in order to ensure that a diverse electrophile scope was evaluated. This approach to select diverse electrophiles covering chemical space enables the assessment of the generality and limitations of this method.

Notably, some clusters were oversampled due to availability, cluster size, and chemists' interest, while other clusters included only a single example due to lack of availability or modest cluster size.

The selection of electrophiles was examined for effectiveness using the reaction conditions optimized with phenylsulfonimi-

Table 1. Optimization of Reaction Conditions^a

entry	solvent	base	conv (%)	3aa (%) ^b	er ^c	4aa (%) ^b
1	TBME	Et ₃ N	100	96	90:10	2
2	TBME	DMAEE	100	96	85:15	1
3	TBME	NMM	91	91	80:20	4
4	TBME	DIPEA	99	93	94:6	5
5	1,4-Dioxane	DIPEA	100	97	91:9	1
6	MeTHF	DIPEA	100	95	91:9	1
7	MeCN	DIPEA	100	99	89:11	1
8	Toluene	DIPEA	97	86 (84) ^d	96:4	11

^aConditions: **1a** (1.00 mmol, 1.00 equiv), **2a** (0.98 mmol, 0.98 equiv), Pd₂dba₃ (0.025 mmol, 2.5 mol %), SL-M003-1 (0.050 mmol, 5.0 mol %), and base (3.0 mmol, 3.0 equiv) in solvent (20 mL, 0.05 M) and 100 psi CO at 20 °C. ^bArea % as determined by SFC analysis. ^cEnantiomeric ratio (er) of product in the crude reaction mixture as determined by chiral SFC analysis. ^dIsolated yield after chromatographic purification.

amide **1a** and the Mandyphos SL-M003-1 ligand (Figure 3A). The model electrophile substrate 1-iodonaphthalene **2a** resides in cluster 1 along with other fused aryl iodides such as **2b** that furnished the cross-coupled products **3aa** and **3ab** in 84% and 82% isolated yield and 97:3 and 93:7 er after recrystallization, respectively. A high-quality single crystal was obtained for **3aa** to enable determination of its absolute stereochemical configuration by X-ray crystallography. Cluster 2 includes aryl iodides with *para*-substituted electron-donating groups as well as heteroaryl iodides with distal heteroatoms. Several aryl and heteroaryl electrophiles were selected from this cluster and found to generate products with high enantioselectivity ($\geq 90:10$ er) and excellent chemoselectivity ($\leq 1\%$ bis-acylation). *para*-Methoxy and *para*-morpholino iodobenzenes led to **3ac** and **3ae** in 97:3 and 96:4 er, respectively, in 78–82% yields. The absolute stereochemical configuration of (*R*)-**3ae** was determined from a high-quality single crystal by X-ray crystallography. Similarly high selectivity was observed with 3-iodothiophene **2d** (**3ad** with 78% yield, 97:3 er), while a slightly lower er was obtained with 3-iodopyridine **2f** (**3af** with 84% yield, 90:10 er). Cluster 3 contains electrophiles bearing distal electron-withdrawing functional groups. *para*-CF₃ phenyl and 6-benzothiazole were selected and generated carbonylation products **3ag** and **3ah** with 95:5 and 91:9 er, respectively. Although the latter electrophile led to lower chemoselectivity (13% bis-acylation), both reactions gave satisfactory yields upon isolation (72–73%). Cluster 4 also features electron-deficient aryl iodides represented by reactions forming **3ai** and **3ah**. These reactions show tolerance of ester and bromide substitution, giving excellent performance with 95:5 er, <1% bis-acylation, and 84–90% yields.

Steric hindrance presented by aryl and heteroaryl iodides with *ortho*-substituents challenges the effectiveness of this cross-coupling. *ortho*-Methyl (**2k**) and *ortho*-phenyl (**2l**) substituted aryl iodides led to products with good enantio- and chemoselectivity (94:6 er and 90:10 er, respectively),

albeit sluggish reactivity, with low conversions (50–74%) and consequently modest isolated yields (32–40%). In contrast, aryl iodides with strongly electron-donating groups in the *ortho* position such as NHBOC (**2m**) and OMe (**2n**) remained effective (80–86% isolated yield) and proceeded with comparable enantioselectivity (84:16 to 90:10 er). While the chemoselectivity with the *ortho*-methoxy substituent is poor (92% bis-acylation) under the standard conditions, using toluene as the solvent, a more chemoselective coupling (23% bis-acylation) can be achieved with 1,4-dioxane as the solvent to furnish **3an** in moderate yield and er. Similarly, 2-iodo-4-nitroanisole **2o** features an *ortho*-methoxy group in addition to a *meta*-electron-withdrawing group. Under the standard conditions, the cross-coupling to give **3ao** occurred with high bis-acylation (91%), which was similarly successfully remedied by conducting the reaction in 1,4-dioxane to afford **3ao** in 70% yield with 78:22 er.

The reaction tolerated 2,3-dichloro (**3ap** with 65% yield, 89:11 er) and 2-bromo-4-fluoro (**3aq** with 25% yield, 88:12 er) substitution but failed to produce the desired products with three 2,6-substituted aryl iodides (**2r–t**) from cluster 9. Bis-*ortho* substitution appears to be a limitation of this method, as bis-*ortho*-fluoro substituents **2v** give modest yield and enantioselectivity (34%, 77:23 er). As seen previously, a single *ortho*-substituent is well tolerated, with *N*-Boc 3-iodo-1*H*-indole undergoing carbonylation smoothly to form **3au** with excellent enantioselectivity and chemoselectivity.

Finally, clusters 11–13 are composed of heteroaryl iodides, with at least one heteroatom *ortho* to the iodide substituent. Subjecting 5-iodo-1-methyl-1*H*-pyrazole to the cross-coupling protocol furnished product **3aw** with high enantioselectivity (94:6 er) with modest bis-acylation (21%). Upon purification, single-crystal X-ray diffraction of **3aw** corroborated the previously assigned absolute configuration as (*R*). Reactivity with 7-chloro-2-iodothieno[3,2-*b*]pyridine gave **3ax** in moderate enantioselectivity (81:19 er), but with low bis-acylation (3%). This further emphasizes that the Pd catalyst remains highly selective toward aryl iodides even in the presence of activated aryl chlorides or bromides. Despite being an activated aryl iodide, no reaction was observed for 2-iodopyridazine **2y**. Overall, electrophiles representing 11 of the 13 total clusters were found to be viable substrates for this asymmetric aryl-carbonylative cross-coupling, indicating a robust transformation that tolerates a wide range of functional groups. Additionally, attempts to quantitatively correlate enantioselectivity to computationally derived molecular features were unsuccessful, as the relatively flat response surface (poor range and statistical spread of the er) rendered this process difficult. Importantly, in many cases, the enantiomeric excess was upgraded through the purification process via crystallization or trituration.

Sulfonimidamide Substrate Scope Exploration. We subsequently investigated the sulfonimidamide substrate scope. Principal component analysis (PCA) was employed to visualize the synthetically feasible sulfonimidamide chemical space using DFT-derived molecular descriptors (SI for details) (Figure 4A). PCA was selected as a dimensionality reduction technique for visualization due to the limited examples of readily accessible sulfonimidamides, as this technique provides for a simpler interpretation of the chemical space (wherein similarity is derived from Euclidian distance). Ultimately, a set of examples was qualitatively selected for synthesis and submission to the previously optimized reaction conditions

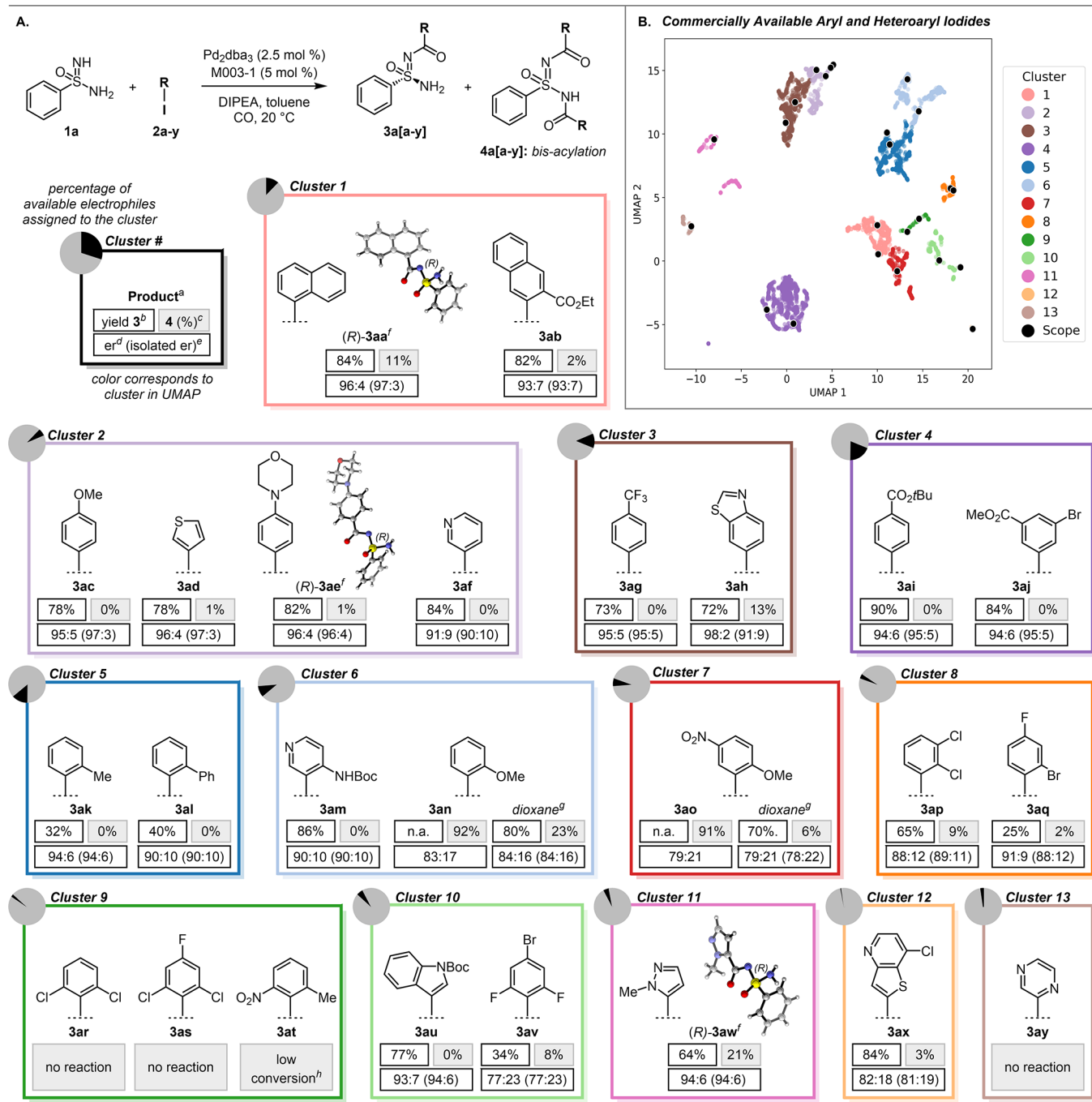


Figure 3. Exploration of the electrophile scope. (A) Electrophile scope separated by clusters. Pie charts indicate the percentage of commercially available aryl and heteroaryl iodides assigned to the specific cluster; border colors correspond to cluster number on UMAP. ^aConditions: **1a** (1.00 mmol, 1.00 equiv), **2** (0.98 mmol, 0.98 equiv), Pd_2dba_3 (0.025 mmol, 2.5 mol %), SL-M003-1 (0.050 mmol, 5.0 mol %), and DIPEA (3.0 mmol, 3.0 equiv) in toluene (20 mL, 0.05 M) and 100 psi of CO at 20 °C. ^bIsolated yield after purification. ^cPercentage relative to corresponding product **3** only (by SFC analysis after normalizing to 100%). ^der of product in the crude reaction mixture as determined by chiral SFC analysis. ^eer of isolated product following reslurry/trituration as determined by chiral SFC analysis. ^fAbsolute configuration as determined by X-ray crystallographic analysis. ^gReactions performed in 1,4-dioxane. ^hTrace product was detected by SFC-MS analysis. The er could not be determined accurately due to poor minor enantiomer peak intensity. Product was not isolated. (B) UMAP representation of commercially available aryl and heteroaryl iodides (5172 total electrophiles) colored by clusters, which were generated using Ward clustering (number of clusters = 13). Tested electrophiles are indicated by black circles.

using 1-iodonaphthalene **2a** and the Mandyphos SL-M003-1 ligand (Figure 4B). Unprotected sulfonimidamide **1b** was found to give lower enantioselectivity (93:7 er) but similar chemoselectivity (10% bis-acylation) to the model substrate **1a**. Isolation of the material through recrystallization in toluene

resulted in an isolated yield of 72% with an upgraded >99:1 er of the desired product **3ba**. The electron-deficient substrate **1c** likewise generated the monoacylated product in lower enantioselectivity (89:11 er) and less bis-acylation (4%). In contrast, carbonylation of electron-rich 4-methoxy substrate **1d**

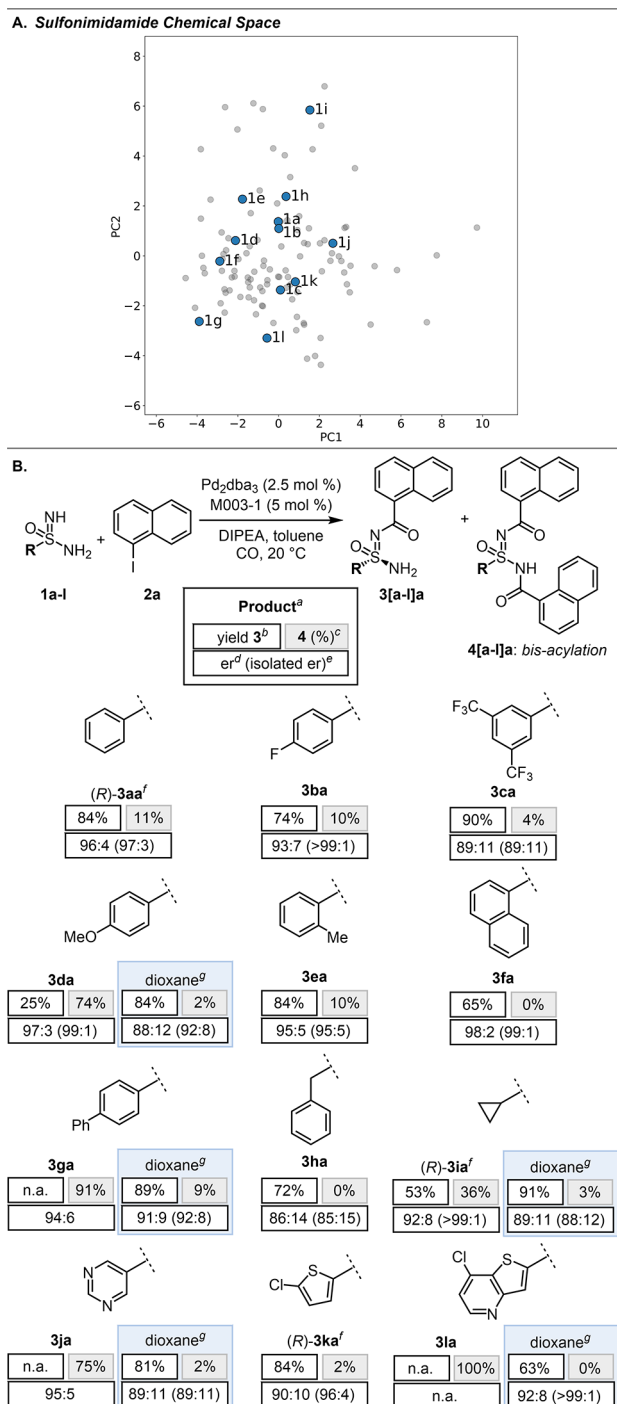


Figure 4. Exploration of the sulfonimidamide substrate scope. (A) PCA of synthetically feasible sulfonimidamides (43.7% of the total variance depicted with 2 principal components), selected substrates indicated in blue. (B) Sulfonimidamide substrate scope. ^aStandard reaction conditions: 1 (1.00 mmol, 1.00 equiv), 2a (0.98 mmol, 0.98 equiv), Pd_2dba_3 (0.025 mmol, 2.5 mol %), SL-M003-1 (0.050 mmol, 5.0 mol %), and DIPEA (3.0 mmol, 3.0 equiv) in toluene (20 mL, 0.05 M) and 100 psi of CO at 20 °C. ^bIsolated yield after purification. ^cPercentage relative to corresponding product 3 only (by SFC analysis after normalizing to 100%). ^der of product in the crude reaction mixture as determined by chiral SFC analysis. ^eer of isolated product following reslurry/trituration as determined by chiral SFC analysis. ^fAbsolute configuration as determined by X-ray crystallographic analysis. ^gReactions performed in 1,4-dioxane.

led to high enantioselectivity (97:3 er), albeit with a concomitant increase in bis-acylation (74%). Conducting the reaction in 1,4-dioxane modulates the bis-acylation reaction to give higher yields of product 3da (84%) but with a slight reduction in enantioenrichment (92:8 er). The reaction is furthermore tolerant of *ortho*-substituted arenes at sulfur (1e and 1f), giving high enantioselectivities (95:5 and 99:1 er, respectively). A lower yield was obtained for the latter due to incomplete conversion (65%). A *para*-biphenyl substituted 1g and aliphatic substituted sulfonimidamides (1h and 1i) were found to give good chemoselectivity (0–9% bis-acylation) and enantioselectivity (85:15 to 92:8 er). Heterocyclic substituents at sulfur (1j, 1k, and 1l) were also tolerated in the carbonylative cross-coupling with moderate to high enantioselectivities (89:11 to >99:1 er). Disparate degrees of bis-acylation were initially observed for 1j and 1l in toluene, but conducting the reaction in 1,4-dioxane promoted the selective formation of monoacylated products ($\leq 2\%$ bis-acylation). Overall, this reaction tolerates a diverse array of sulfonimidamides bearing aryl, benzyl, alkyl, and heterocyclic substitution with generally high stereoselectivity ($\geq 85:15$ er). Many resulting products were also crystalline, and thus, X-ray crystallographic analysis was utilized to confirm the absolute configuration of 3aa, 3ia, and 3ka as (R).

Further Synthetic Transformations. With a library of enantioenriched monoacylated sulfonimidamides in hand, we then evaluated the synthetic versatility of these materials. While numerous transformations of sulfonimidamides have been previously documented, many of these reactions were conducted on racemic mixtures due to limited technologies for their asymmetric synthesis.³¹ We envisioned that the enantioenrichment at sulfur should be maintained throughout a suite of reactions and, as such, explored this question to demonstrate the value of acyl sulfonimidamides as enantioenriched intermediates.

Pleasingly, sulfonimidamide 3aa reacted with 4-chlorophenyl isocyanate to form urea 5 in 82% yield while largely preserving enantiomeric enrichment at sulfur (94:6 er) (Figure 5a).³² Similarly, a Mitsunobu reaction to form a piperidyl heterocyclic substituent at sulfur was successful when performed with 1,5-pentanediol (6, 69%, 97:3 er) (Figure 5b).³³ Furthermore, we found 3aa to be effective as a nucleophile in a Cu-catalyzed N-arylation with 4-iodotoluene, producing 7 in 83% yield while preserving the starting material's high enantiomeric enrichment (94:6 er) (Figure 5c).³⁴ Finally, we utilized sulfonimidamide 3ka, an analog of the oncolytic compound presented in Figure 1A, as an electrophile in a Suzuki–Miyaura coupling with 4-fluorophenylboronic acid to demonstrate further derivatization, achieving an 89% yield of product 8 with good enantiomeric retention (89:11 er) (Figure 5d).³⁵ These transformations, while far from exhaustive, demonstrate the utility of the products accessed in this study.

CONCLUSIONS

We have developed a Pd-catalyzed enantioselective aryl-carbonylation to access enantioenriched sulfonimidamides and provided a promising path to advance the asymmetric functionalization of sulfonimidamides. Chemical space analysis guided the initial ligand training set design, which enabled the rapid identification of an optimal catalyst. This training set design should provide a blueprint for future efforts to evaluate new asymmetric reactions using chiral bisphosphines. The

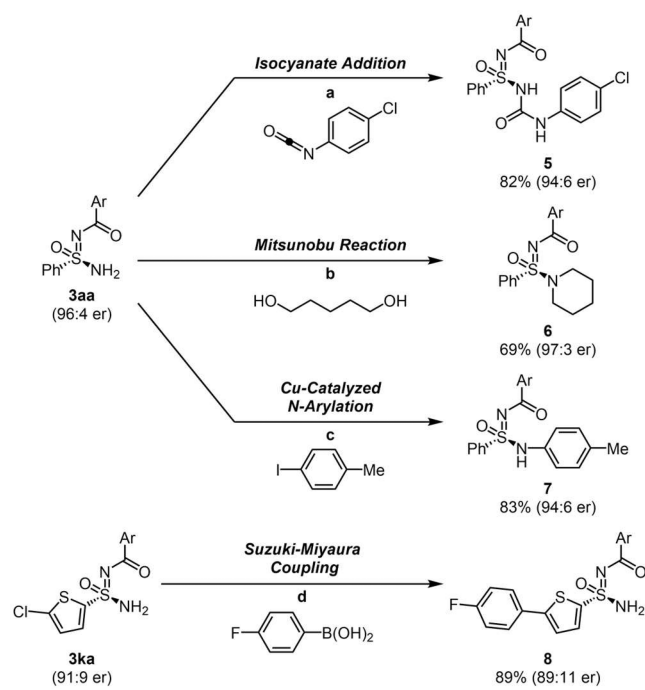


Figure 5. Synthetic versatility of acyl sulfonimidamides. Ar = 1-naphthyl. (a) 3aa (0.50 mmol, 1 equiv), 4-chlorophenyl isocyanate (0.55 mmol, 1.1 equiv), and NMM (1.0 mmol, 2 equiv) in DCM (2.5 mL, 0.2 M) at 0 → 25 °C. (b) 3aa (0.50 mmol, 1 equiv), 1,5-pentanediol (0.6 mmol, 1.2 equiv), PPh₃ (1.15 mmol, 2.3 equiv), and diisopropyl azodicarboxylate (DIAD) (1.05 mmol, 2.1 equiv) in THF (10 mL, 0.05 M) at 0 → 25 °C. (c) 3aa (0.50 mmol, 1 equiv), CuCl (0.075 mmol, 15 mol %), DMEDA (0.10 mmol, 20 mol %), K₂CO₃ (1.25 mmol, 2.5 equiv), and 4-iodotoluene (0.55 mmol, 1.1 equiv) in DMSO (1.25 mL, 0.4 M) at 80 °C. (d) 3ka (0.25 mmol, 1 equiv), Pd₂dba₃ (0.005 mmol, 2 mol %), XPhos (0.01 mmol, 4 mol %), K₂CO₃ (0.50 mmol, 2 equiv), and 4-fluorophenylboronic acid (0.33 mmol, 1.3 equiv) in *n*-BuOH (0.5 mL, 0.5 M) at 80 °C.

substrate scope selection was also motivated by chemical space exploration in order to systematically assess the generality of this method, further emphasizing the role of data science in synthetic chemistry. Using these tools, we demonstrated that a wide variety of aryl and heteroaryl iodides are tolerated along with a diverse range of unprotected, racemic sulfonimidamides. We foresee that this Pd-catalyzed cross-coupling method for the asymmetric synthesis of sulfonimidamides will find application in medicinal chemistry, agrochemical discovery, and academic research.

ASSOCIATED CONTENT

Supporting Information

The Supporting Information is available free of charge at <https://pubs.acs.org/doi/10.1021/jacs.3c06674>.

Aryl iodide descriptors ([XLSX](#))

Sulfonimidamide descriptors ([XLSX](#))

Detailed experimental procedures, compound characterization data, and computational methods are also available ([PDF](#))

Accession Codes

CCDC 2271982, 2271984–2271986, and 2271994 contain the supplementary crystallographic data for this paper. These data can be obtained free of charge via www.ccdc.cam.ac.uk/data_request/cif, or by emailing data_request@ccdc.cam.ac.

uk, or by contacting The Cambridge Crystallographic Data Centre, 12 Union Road, Cambridge CB2 1EZ, UK; fax: +44 1223 336033.

AUTHOR INFORMATION

Corresponding Authors

Ngiap-Kie Lim — Department of Small Molecule Process Chemistry, Genentech, Inc., South San Francisco, California 94080, United States; orcid.org/0000-0002-3760-4874; Email: lim.ngiapkie@gene.com

F. Dean Toste — Department of Chemistry, University of California, Berkeley, California 94720, United States; orcid.org/0000-0001-8018-2198; Email: fdtoste@berkeley.edu

Matthew S. Sigman — Department of Chemistry, University of Utah, Salt Lake City, Utah 84112, United States; orcid.org/0000-0002-5746-8830; Email: matt.sigman@utah.edu

Authors

Lucy van Dijk — Department of Chemistry, University of Utah, Salt Lake City, Utah 84112, United States; orcid.org/0000-0002-1899-087X

Brittany C. Haas — Department of Chemistry, University of Utah, Salt Lake City, Utah 84112, United States; orcid.org/0000-0001-5344-4375

Kyle Clagg — Department of Small Molecule Process Chemistry, Genentech, Inc., South San Francisco, California 94080, United States

Jordan J. Dotson — Department of Small Molecule Process Chemistry, Genentech, Inc., South San Francisco, California 94080, United States

Sean M. Treacy — Department of Chemistry, University of California, Berkeley, California 94720, United States

Katarzyna A. Piechowicz — Department of Small Molecule Process Chemistry, Genentech, Inc., South San Francisco, California 94080, United States

Vladislav A. Roytman — Department of Chemistry, University of California, Berkeley, California 94720, United States

Haiming Zhang — Department of Small Molecule Process Chemistry, Genentech, Inc., South San Francisco, California 94080, United States; orcid.org/0000-0002-2139-2598

Scott J. Miller — Department of Chemistry, Yale University, New Haven, Connecticut 06511, United States; orcid.org/0000-0001-7817-1318

Francis Gosselin — Department of Small Molecule Process Chemistry, Genentech, Inc., South San Francisco, California 94080, United States; orcid.org/0000-0001-9812-4180

Complete contact information is available at:

<https://pubs.acs.org/10.1021/jacs.3c06674>

Author Contributions

#L.V.D. and B.C.H. contributed equally to this work.

Notes

The authors declare no competing financial interest.

The full bisphosphine ligand descriptor library and Python scripts used for bisphosphine ligand chemical space analysis have been made available: https://github.com/SigmanGroup/Multiobjective_Optimization.

ACKNOWLEDGMENTS

We thank Karissa Cruz, Catherine Capitana, Steven Chin, Dr. David Russell, Dr. Jose Napolitano, Dr. Cris Crittenden, and Dr. Kenji Kurita for analytical support; Colin Masui and Adam Childs for performing high-throughput experimentation; Dr. Antonio DiPasquale for X-ray crystallographic support; Wendy Williams for assistance with the aryl iodide libraries; and Dr. Kyle Mack, Dr. Richard Walroth, Dr. Jacob Timmerman, and Dr. Janis Jermaks for helpful discussions. M.S.S., F.D.T., and L.v.D. acknowledge financial support from the NSF under the CCI Center for Computer Assisted Synthesis (CHE-1925607 and CHE-2202693). J.J.D. acknowledges financial support from the NIH (F32-GM140529). The computational portion of this work was supported by the Center for High Performance Computing at the University of Utah. We thank Dr. Hasan Celik and UC Berkeley's NMR facility in the College of Chemistry (CoC-NMR) for spectroscopic assistance. Instruments at the CoC-NMR are supported in part by NIH S10OD024998.

REFERENCES

- (1) Domagk, G. Chemotherapie der Streptokokken-Infektionen. *Klinische Wochenschrift* **1936**, *15*, 1585–1590.
- (2) Zhao, C.; Rakesh, K. P.; Ravidar, L.; Fang, W. Y.; Qin, H. L. Pharmaceutical and medicinal significance of sulfur (SVI)-Containing motifs for drug discovery: A critical review. *Eur. J. Med. Chem.* **2019**, *162*, 679–734.
- (3) Chinthakindi, P. K.; Naicker, T.; Thota, N.; Govender, T.; Kruger, H. G.; Arvidsson, P. I. Sulfonimidamides in Medicinal and Agricultural Chemistry. *Angew. Chem., Int. Ed.* **2017**, *56*, 4100–4109.
- (4) Sehgelmeble, F.; Janson, J.; Ray, C.; Rosqvist, S.; Gustavsson, S.; Nilsson, L. I.; Minidis, A.; Holenz, J.; Rotticci, D.; Lundkvist, J.; Arvidsson, P. I. Sulfonimidamides as Sulfonamides Bioisosteres: Rational Evaluation through Synthetic, in Vitro, and in Vivo Studies with γ -Secretase Inhibitors. *ChemMedChem.* **2012**, *7*, 396–399.
- (5) Zhang, Z.-X.; Willis, M. C. Sulfonimidamides as new functional groups for synthetic and medicinal chemistry. *Chem.* **2022**, *8*, 1137–1146.
- (6) Examples from the patent literature: (a) Biftu, T.; Khan, T. A. Treating diabetes with dipeptidyl peptidase-IV inhibitors. WO2014/018355A1, 2014. (b) Langkopf, E.; Blum, A. Azabenzimidazole derivatives as AMP protein kinase agonists. WO2016/023789A1, 2016. (c) Chowdhury, S.; Dehnhardt, C. M.; Focken, T.; Grimwood, M. E.; Hemeon, I. W.; Mckerrall, S.; Sutherlin, D. Substituted benzamides and methods of use thereof. WO2017/172802A1, 2017. (d) Trainor, G. L. Tricyclic modulators of PP2A. WO2021/170913A1, 2021.
- (7) Chen, Y.; Gibson, J. A convenient synthetic route to sulfonimidamides from sulfonamides. *RSC Adv.* **2015**, *5*, 4171–4174.
- (8) Gao, B.; Li, S.; Wu, P.; Moses, J. E.; Sharpless, K. B. SuFEx Chemistry of Thionyl Tetrafluoride (SOF_4) with Organolithium Nucleophiles: Synthesis of Sulfonimidoyl Fluorides, Sulfoximines, Sulfonimidamides, and Sulfonimidates. *Angew. Chem., Int. Ed.* **2018**, *57*, 1939–1943.
- (9) Worch, C.; Atodiresei, I.; Raabe, G.; Bolm, C. Synthesis of Enantiopure Sulfonimidamides and Elucidation of Their Absolute Configuration by Comparison of Measured and Calculated CD Spectra and X-Ray Crystal Structure Determination. *Chem. Eur. J.* **2010**, *16*, 677–683.
- (10) Greed, S.; Briggs, E. L.; Idiris, F. I. M.; White, A. J. P.; Lücking, U.; Bull, J. A. Synthesis of Highly Enantioenriched Sulfonimidoyl Fluorides and Sulfonimidamides by Stereospecific Sulfur–Fluorine Exchange (SuFEx) Reaction. *Chem. Eur. J.* **2020**, *26*, 12533–12538.
- (11) Wojaczyńska, E.; Wojaczyński, J. Modern Stereoselective Synthesis of Chiral Sulfanyl Compounds. *Chem. Rev.* **2020**, *120*, 4578–4611.
- (12) Liang, C.; Collet, F.; Robert-Peillard, F.; Müller, P.; Dodd, R. H.; Dauban, P. Toward a Synthetically Useful Stereoselective C–H Amination of Hydrocarbons. *J. Am. Chem. Soc.* **2008**, *130*, 343–350.
- (13) Tilby, M. J.; Dewez, D. F.; Hall, A.; Martínez Lamenza, C.; Willis, M. C. Exploiting Configurational Lability in Aza-Sulfur Compounds for the Organocatalytic Enantioselective Synthesis of Sulfonimidamides. *Angew. Chem., Int. Ed.* **2021**, *60*, 25680–25687.
- (14) Zhang, X.; Wang, F.; Tan, C.-H. Asymmetric Synthesis of S(IV) and S(VI) Stereogenic Centers. *JACS Au* **2023**, *3*, 700–714.
- (15) Yang, G.-f.; Yuan, Y.; Tian, Y.; Zhang, S.-q.; Cui, X.; Xia, B.; Li, G.-x.; Tang, Z. Synthesis of Chiral Sulfonimidoyl Chloride via Desymmetrizing Enantioselective Hydrolysis. *J. Am. Chem. Soc.* **2023**, *145*, 5439–5446.
- (16) Borhade, S. R.; Sandström, A.; Arvidsson, P. I. Synthesis of Novel Aryl and Heteroaryl Acyl Sulfonimidamides via Pd-Catalyzed Carbonylation Using a Nongaseous Precursor. *Org. Lett.* **2013**, *15*, 1056–1059.
- (17) Wakchaure, P. B.; Borhade, S. R.; Sandström, A.; Arvidsson, P. I. Synthesis of Vinyl- and Aryl–Acyl Sulfonimidamides Through Pd-Catalyzed Carbonylation Using $\text{Mo}(\text{CO})_6$ as ex situ CO Source. *Eur. J. Org. Chem.* **2015**, *2015*, 213–219.
- (18) Dotson, J. J.; van Dijk, L.; Timmerman, J. C.; Grosslight, S.; Walroth, R. C.; Gosselin, F.; Püntener, K.; Mack, K. A.; Sigman, M. S. Data-Driven Multi-Objective Optimization Tactics for Catalytic Asymmetric Reactions Using Bisphosphine Ligands. *J. Am. Chem. Soc.* **2023**, *145*, 110–121.
- (19) Zahrt, A. F.; Rose, B. T.; Darrow, W. T.; Henle, J. J.; Denmark, S. E. Computational Methods for Training Set Selection and Error Assessment Applied to Catalyst Design: Guidelines for Deciding Which Reactions to Run First and Which to Run Next. *React. Chem. Eng.* **2021**, *6*, 694–708.
- (20) See, X. Y.; Wen, X.; Wheeler, T. A.; Klein, C. K.; Goodpaster, J. D.; Reiner, B. R.; Tonks, I. A. Iterative Supervised Principal Component Analysis Driven Ligand Design for Regioselective Ti-Catalyzed Pyrrole Synthesis. *ACS Catal.* **2020**, *10*, 13504–13517.
- (21) Gensch, T.; Smith, S. R.; Colacot, T. J.; Timsina, Y.; Xu, G.; Glasspoole, B. W.; Sigman, M. S. Design and Application of a Screening Set for Monophosphine Ligands in Cross-Coupling. *ACS Catal.* **2022**, *12*, 7773–7780.
- (22) Kariofillis, S. K.; Jiang, S.; Zuranski, A. M.; Gandhi, S. S.; Martinez Alvarado, J. I.; Doyle, A. G. Using Data Science To Guide Aryl Bromide Substrate Scope Analysis in a Ni/Photoredox-Catalyzed Cross-Coupling with Acetals as Alcohol-Derived Radical Sources. *J. Am. Chem. Soc.* **2022**, *144*, 1045–1055.
- (23) Felten, S.; He, C. Q.; Weisel, M.; Shevlin, M.; Emmert, M. H. Accessing Diverse Azole Carboxylic Acid Building Blocks via Mild C–H Carboxylation: Parallel, One-Pot Amide Couplings and Machine-Learning-Guided Substrate Scope Design. *J. Am. Chem. Soc.* **2022**, *144*, 23115–23126.
- (24) Knochel, P.; Schwink, L. A New Practical Asymmetric Synthesis of C₂-Symmetrical 1,1'-Ferrocenyl Diols via CBS-Reduction. *Tetrahedron Lett.* **1996**, *37*, 25–28.
- (25) Spindler, F.; Malan, C.; Lotz, M.; Kesselgruber, M.; Pittelkow, U.; Rivas-Nass, A.; Briel, O.; Blaser, H.-U. Modular chiral ligands: the profiling of the Mandyphos and Taniaphos ligand families. *Tetrahedron Asymm.* **2004**, *15*, 2299–2306.
- (26) Sun, X.; Zhou, L.; Li, W.; Zhang, X. Convenient Divergent Strategy for the Synthesis of TunePhos-Type Chiral Diphosphine Ligands and Their Applications in Highly Enantioselective Ru-Catalyzed Hydrogenations. *J. Org. Chem.* **2008**, *73*, 1143–1146.
- (27) Schmid, R.; Foricher, J.; Cereghetti, M.; Schonhoizer, P. Axially Dissymmetric Diphosphines in the Biphenyl Series: Synthesis of (6,6'-Dimethoxybiphenyl-2,2'-diyl)bis(diphenylphosphine) ('MeO-BIPHEP') and Analogues via an *ortho*-Lithiation/Iodination Ullmann-Reaction Approach. *Helv. Chim. Acta* **1991**, *74*, 370–389.
- (28) Haas, B. C.; Goetz, A. G.; Bahamonde, A.; McWilliams, J. C.; Sigman, M. S. Predicting relative efficiency of amide bond formation using multivariate linear regression. *Proc. Natl. Acad. Sci. U. S. A.* **2022**, *119*, No. e2118451119.

(29) Tang, T.; Hazra, A.; Min, D. S.; Williams, W. L.; Jones, E.; Doyle, A. G.; Sigman, M. S. Interrogating the Mechanistic Features of Ni(I)-Mediated Aryl Iodide Oxidative Addition Using Electroanalytical and Statistical Modeling Techniques. *J. Am. Chem. Soc.* **2023**, *145*, 8689–8699.

(30) Zuranski, A. M.; Wang, J. Y.; Shields, B. J.; Doyle, A. G. Auto-QChem: an automated workflow for the generation and storage of DFT calculations for organic molecules. *React. Chem. Eng.* **2022**, *7*, 1276–1284.

(31) Nandi, G. C.; Arvidsson, P. I. Sulfonimidamides: Synthesis and Applications in Preparative Organic Chemistry. *Adv. Synth. Catal.* **2018**, *360*, 2976–3001.

(32) Chen, Y.; Söderlund, J.; Grönberg, G.; Pettersen, A.; Aurell, C.-J. Synthesis of 1 λ ,2,4,6-Thiatriazine-1,3,5-Trione Derivatives. *Eur. J. Org. Chem.* **2019**, *2019*, 4731–4740.

(33) Azzaro, S.; Fensterbank, L.; Lacôte, E.; Malacria, M. Probing the Amino-End Reactivity of Sulfonimidamides. *Synlett* **2008**, *2008*, 2253–2256.

(34) Azzaro, S.; Desage-El Murr, M.; Fensterbank, L.; Lacôte, E.; Malacria, M. Copper-Catalyzed N-Arylation of Sulfonimidamides. *Synlett* **2011**, *2011*, 849–851.

(35) Billingsley, K.; Buchwald, S. L. Highly Efficient Mono-phosphine-Based Catalyst for the Palladium-Catalyzed Suzuki–Miyaura Reaction of Heteroaryl Halides and Heteroaryl Boronic Acids and Esters. *J. Am. Chem. Soc.* **2007**, *129*, 3358–3366.

■ NOTE ADDED AFTER ASAP PUBLICATION

This paper published ASAP on September 1, 2023 with a production error in the rendering of Figures 2, 3, and 4. The figures were corrected and the revised manuscript reposted on September 5, 2023.